Proteome-wide Profiling of Isoniazid Targets in *Mycobacterium tuberculosis*†

Argyrides Argyrou,‡,§ Lianji Jin,|| Linda Siconilfi-Baez,|| Ruth H. Angeletti,|| and John S. Blanchard*,‡

Department of Biochemistry, Albert Einstein College of Medicine, 1300 Morris Park Avenue, Bronx, New York 10461, and Laboratory for Macromolecular Analysis and Proteomics, Albert Einstein College of Medicine, 1300 Morris Park Avenue, Bronx, New York 10461

Received September 8, 2006; Revised Manuscript Received October 19, 2006

ABSTRACT: Isoniazid (INH) is an essential drug used to treat tuberculosis. The mycobactericidal agents are INH adducts [INH−NAD(P)] of the pyridine nucleotide coenzymes, which are generated in vivo after INH activation and which bind to, and inhibit, essential enzymes. The NADH-dependent enoyl-ACP reductase (InhA) and the NADPH-dependent dihydrofolate reductase (DfrA) have both been shown to be inhibited by INH−NAD(P) adducts with nanomolar affinity. In this paper, we profiled the *Mycobacterium tuberculosis* proteome using both the INH−NAD and INH−NADP adducts coupled to solid supports and identified, in addition to InhA and DfrA, 16 other proteins that bind these adducts with high affinity. The majority of these are predicted to be pyridine nucleotide-dependent dehydrogenases/reductases. They are involved in many cellular processes, including *S*-adenosylmethionine-dependent methyl transfer reactions, pyrimidine and valine catabolism, the arginine degradative pathway, proton and potassium transport, stress response, lipid metabolism, and riboflavin biosynthesis. The targeting of multiple enzymes could, thus, account for the pleiotropic effects of, and powerful mycobactericidal properties of, INH.

The powerful and specific antitubercular effects of isoniazid [isonicotinic acid hydrazide (INH)][1] were discovered in 1952, and revolutionized the treatment of tuberculosis (*1*−*3*). INH continues to be extensively used in the treatment of the disease to this day, singly in prophylaxis or in a multidrug combination with rifampicin, pyrazinamide, and ethambutol for active infections.

The mechanism by which this simple compound exerts its powerful effect on *Mycobacterium tuberculosis* [minimum inhibitory concentration (MIC) of 0.02−0.05 μg/mL] began to be unraveled in the early 1990s shortly after genetic tools for mycobacteria were being developed. Strains of *M. tuberculosis* and *Mycobacterium smegmatis* that were resistant to high levels of INH were first shown to have deletions or point mutations in the *katG* gene, which led to the proposal that INH was a pro-drug that was oxidatively activated by the *katG*-encoded mycobacterial catalase-peroxidase (*4*). In a second genetic study, a spontaneous *M. smegmatis* mc^2155 mutant and a *Mycobacterium bovis* BCG mutant that were coresistant to INH and ethionamide, a structural analogue of INH, were both shown to have a point mutation (S94A) in the *inhA*-encoded enoyl-ACP reductase (*5*). Furthermore, resistance was observed through overexpression of wild-type InhA or the S94A mutant in *M. smegmatis* mc^2155, which led to the identification of InhA as a target for INH (*5*).

A consensus about the mechanism of action of, and resistance to, INH has emerged over the past few years. The oxidation of INH by KatG generates an isonicotinoyl radical that reacts nonenzymatically with cellular pyridine nucleotides to generate an ensemble of isonicotinoyl−NAD(P) adducts [INH−NAD(P) (Figure 1)] (*6*). Of the 12 possible adducts of INH, only two have thus far been shown to inhibit essential enzymes. The acyclic 4*S* isomer of INH-NAD (compound **1**, Figure 1) is known to be a slow-onset, tight-binding inhibitor of InhA (K_i* = 1 nM) (*7*, *8*). Inhibition of InhA prevents the elongation of C_{26} fatty acids by the fatty acid synthase II complex (*9*, *10*) and prevents the formation of the mycolic acids that are an important defense against the host immune surveillance and defense system (*11*, *12*). We have recently demonstrated that the acyclic 4*R* isomer of the INH−NADP adduct (compound **4**, Figure 1) inhibits the *dfrA*-encoded dihydrofolate reductase (DHFR) with subnanomolar affinity and acts as a bisubstrate analogue (*13*). DHFR maintains the cellular pool of folic acid in the four-electron reduced form by catalyzing the NADPH-dependent reduction of dihydrofolate (and folate, albeit less efficiently) to tetrahydrofolate (*14*). By acquiring single-carbon units at the methyl, methylene, and formyl oxidation levels, tetrahydrofolate is an important single-carbon coenzyme donor involved in many important enzymatic reactions, which are

† This work was supported by a National Institutes of Health grant to J.S.B. (AI33396).

* To whom correspondence should be addressed: Department of Biochemistry, Albert Einstein College of Medicine, 1300 Morris Park Ave., Bronx, NY 10461. Telephone: (718) 430-3096. Fax: (718) 430-8565. E-mail: blanchar@aecom.yu.edu.

‡ Department of Biochemistry.

§ Present address: Department of Chemical Enzymology, Bristol-Myers Squibb Pharmaceutical Co., Pharmaceutical Research Institute, P.O. Box 5400, Princeton, NJ 08543-5400.

|| Laboratory for Macromolecular Analysis and Proteomics.

[1] Abbreviations: ACP, acyl carrier protein; DHFR, dihydrofolate reductase; InhA, enoyl-ACP reductase; EDTA, ethylenediaminetetraacetic acid; INH, isonicotinic acid hydrazide (isoniazid); INH−NAD(P), isonicotinoylated nicotinamide adenine dinucleotides; $NAD(P)^+$, oxidized nicotinamide adenine dinucleotide (phosphate); NAD(P)H, reduced nicotinamide adenine dinucleotide (phosphate); Pipes, piperazine-1,4-bis(2-ethanesulfonic acid); SDS−PAGE, sodium dodecyl sulfate−polyacrylamide gel electrophoresis; Tris, tris(hydroxymethyl)-aminomethane.

10.1021/bi061874m CCC: $33.50
Published on Web 11/08/2006

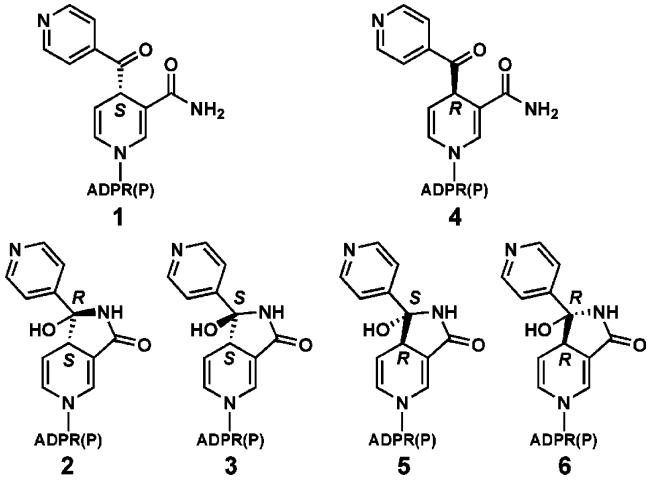

FIGURE 1: Chemical structures of the INH−NAD and INH−NADP adducts. The adenosine diphosphoribose (for INH-NAD) and 2′-phosphoadenosine diphosphoribose (for INH−NADP) moieties of these molecules are abbreviated as ADPR(P). Each of the *R* and *S* acyclic forms is in equilibrium with the corresponding pair of diastereomeric, cyclic, hemiaminal forms. Cyclization occurs by intramolecular attack of the amide nitrogen of the nicotinamide ring on the carbonyl group of the isonicotinoyl moiety (*6*).

necessary for the biosynthesis of nucleic acids, purines, pyrimidines, and several amino acids (*14*).

Clinical resistance to isoniazid has been increasing rapidly, leading to treatment failure and diminished therapeutic outcomes. The appearance of multidrug-resistant tuberculosis (resistance to the two first-line drugs, isoniazid and rifampicin) requires the lengthy use of second-line drugs that are less effective, more toxic, and more costly than the first-line drugs (*15*). Thus, new antitubercular drugs are urgently needed. Effective drug development requires good drug target selection. A powerful way of identifying such targets is to identify the targets of existing effective drugs, such as INH against tuberculosis.

Are there other INH targets? The majority of INH-resistant *M. tuberculosis* clinical isolates have mutations in *katG* or *inhA*; however, 10−25% of these have unknown genotypes (*15*), suggesting that there may be additional targets. In addition, the complete genome sequence of *M. tuberculosis* (*16*) suggests that, like other organisms, there are a large number of pyridine nucleotide-dependent reductases and dehydrogenases with substrates that could be mimicked by INH−NAD(P) adducts acting as bisubstrate analogues of these enzymes.

Although mycobacterial genetics has continued to provide insight into the mechanisms of resistance to INH (*17*−*19*), it has not yet provided any additional INH targets. Genomic (*20*−*24*) and proteomic (*25*) studies have also been employed to identify genes that show altered levels of expression when mycobacteria are treated with INH. However, the RNA and protein levels of KatG, InhA, and DHFR are unaltered after INH treatment, and to date, these studies have failed to provide any new targets for INH. In this paper, we employed the old, but extraordinarily powerful, method of affinity chromatography on solid supports to which the INH−NAD and INH−NADP adducts were coupled to effect the selective purification of those enzymes that bind the INH adducts tightly. In addition to InhA and DHFR, we identified 16 other proteins that bind these adducts tightly. These newly identified proteins are potential candidates for drug development that require further validation, including gene knockout studies to assess essentiality, overexpression of these proteins in *M. tuberculosis* to determine if they can confer resistance to isoniazid by drug sequestration, recombinant protein expression and purification, assay development to confirm or assign function and determine the extent of inhibition of enzyme activity by the INH adducts in vitro, and X-ray crystallography structural studies.

MATERIALS AND METHODS

Determination of Protein Concentrations. Protein concentrations were determined using the bicinchoninic acid assay kit (Pierce) and bovine serum albumin as a standard (*26*).

Synthesis and Purification of the INH−NAD(P) Adduct. The mixture of INH−NAD(P) adducts was synthesized and purified as described previously (*6*, *27*). The A_{260}/A_{324} ratio (an indicator of purity) of the purified products was 3.95−4.00, which is close to the value of 3.94 reported previously for INH−NAD (*28*). The concentration of INH−NAD(P) was determined from an ϵ_{324} of 6900 M^{-1} cm^{-1} reported previously for INH−NAD (*28*).

Preparation of INH−NAD(P)−Sepharose. Three milliliters of *N*-hydroxysuccinamide-activated Sepharose 4 fast flow resin (Amersham Biosciences) was washed with 10 mL of ice-cold 1 mM hydrochloric acid. $NAD(P)^+$ was first covalently attached via the exocyclic adenine amine to the resin by suspending the beads in 10 mL of 100 mM $NAD(P)^+$ dissolved in 100 mM Pipes buffer (pH 7.5). This reaction was allowed to proceed for 20 h at room temperature by end-over-end mixing. Unreacted sites were then blocked by washing the resin twice with 10 mL of 100 mM Tris (pH 8.0) and stored at 4 °C for 24 h. After the samples had been washed thoroughly with 100 mM sodium phosphate (pH 7.5), INH (2 mM) and Mn(III) pyrophosphate (4 mM) were added to the $NAD(P)^+$−Sepharose resin with gentle magnetic stirring to generate the INH−NAD(P) inhibitor. Mn(III) pyrophosphate (*6*) was added in $^1/_{10}$ portions every 2 min (the final resin suspension volume was 15 mL). The INH−NAD(P)−Sepharose suspension was then poured into a 50 mL disposable column (Bio-Rad) and washed extensively with 50 mM sodium phosphate (pH 7.0) containing 100 mM NaCl and 1 mM EDTA (buffer A). The final bed volume of the columns was 2 mL.

Isolation of INH−NAD(P)-Binding Proteins. M. tuberculosis H37Rv whole cell lysate (10 mL of 20 mg/mL protein, generously provided by the Tuberculosis Vaccine Testing and Research Materials Contract of Colorado State University, Fort Collins, CO) was supplemented with two tablets of complete protease inhibitor cocktail (Roche) and 1 mM EDTA and centrifuged at 20000*g* for 30 min at 4 °C. The supernatant was then dialyzed for 2 h against 4 L of buffer A at 4 °C. Half of the dialysate was applied to the INH−NAD(P)−Sepharose column, while the other half was applied to the $NAD(P)^+$−Sepharose control column without flow. The columns were capped; the resin was suspended, and binding of proteins to the resin was allowed to proceed for 2 h at 4 °C by end-over-end mixing. The resin was then allowed to settle, and the chromatography procedure was initiated at room temperature. After the unbound proteins

had been discarded, the columns were washed with 50 mL of buffer A followed by 20 mL of 1 mM NAD(P)$^+$ in buffer A to remove weakly bound dehydrogenases. Two milliliters of 3.5 mM INH−NAD(P) inhibitor was then applied to the columns and the inhibitor allowed to enter the resin. Flow was stopped, and equilibration was allowed to proceed for 1 h. The eluted proteins were collected and combined with the eluate after 4 mL of buffer A was applied to the columns. These combined fractions were then concentrated to 50 μL (~50 μg of total protein) using a centrifugal filter device through a 10 kDa cutoff membrane (Millipore), and the proteins were analyzed by SDS−PAGE followed by silver staining.

Identification of INH−NAD(P)-Binding Proteins. Protein bands were excised from the gels, reduced, alkylated with iodoacetamide, and digested with proteomics-grade trypsin (Promega). The resulting tryptic peptide mixture was then analyzed by liquid chromatography combined with on-line electrospray mass spectrometry. Peptides were separated on a C18 PepMap 100 column (75 μm × 15 cm; Dionex) at a constant flow rate of 250 nL/min as follows: 20 min at 2% B, 15 min linear gradient from 2 to 52% B, and 5 min at 90% B. Solvent A consists of 2% (v/v) acetonitrile and 0.08% (v/v) formic acid, while solvent B consists of 80% (v/v) acetonitrile and 0.1% (v/v) formic acid. The eluent was directly introduced into the electrospray port of a Finnigan LTQ linear ion trap mass spectrometer (Thermo Electron). The mass spectrometry data were acquired in data-dependent mode. The MS survey scan was recorded between *m*/*z* 300 and 2000, which was then followed by MS/MS scans of the three most intense ions. The normalized collision energy was set at 35%, the repeat count of dynamic exclusion at 2, and the exclusion duration at 180 s.

Database Search and Data Analysis. The raw data file was converted into a peaklist using an in-house script (RawFileExtractor) and was then searched against the nonredundant NCBI database for proteins from the *M. tuberculosis* complex using the Mascot search engine. The search criteria were as follows: Two missed cleavages by trypsin were allowed. Carboxamidomethylation of cysteine residues was fixed. Modification of methionine residues by oxidation was allowed to vary. The mass tolerance for the peptide was set at 2 Da, while the MS/MS tolerance was set at 0.8 Da. Positive protein identification requires a minimum of two unique peptides with peptide ion scores that are greater than or equal to the MOWSE score.

RESULTS

Purification of INH−NAD(P)-Binding Proteins. To isolate proteins from *M. tuberculosis* that bind INH−NAD(P) with high affinity, we covalently linked INH−NAD(P) onto column supports and affinity-purified those proteins from *M. tuberculosis* crude soluble cell extracts that bind these adducts with high affinity (Materials and Methods). After the samples had been extensively washed with buffer and either NAD$^+$ or NADP$^+$, specific elution of INH−NAD(P)-binding proteins was accomplished using the same INH−NAD(P) adduct pool that was covalently attached to the columns. From 100 mg of *M. tuberculosis* crude soluble protein cell extract, approximately 50 μg of total protein was recovered from solid supports containing the covalently coupled INH−NAD(P) adducts, representing an approximately 2000-fold enrichment of proteins that were bound to the coupled adducts. Figure 2 shows silver-stained SDS−PAGE gels of the final INH−NAD(P) protein eluates from the NAD(P)$^+$−Sepharose and INH−NAD(P)−Sepharose columns.

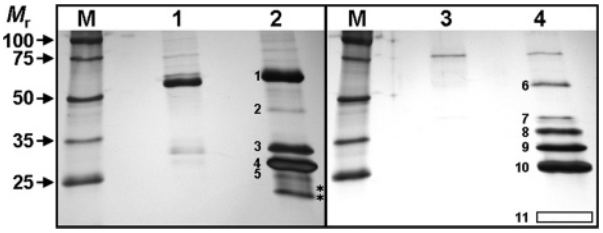

FIGURE 2: SDS−PAGE of the INH−NAD(P) protein eluates from the NAD$^+$−Sepharose (lane 1), INH−NAD−Sepharose (lane 2), NADP$^+$−Sepharose (lane 3), and INH−NADP−Sepharose (lane 4) columns. The gels were silver-stained. The two lanes marked M contained molecular weight markers. The identities of the protein bands marked with numbers are listed in Table 1. The two bands marked with an asterisk (lane 2) correspond to degradation products of band 4 (InhA).

Identification of INH−NAD(P)-Binding Proteins. Protein bands from the INH−NAD(P) protein eluates of the INH−NAD(P)−Sepharose columns were excised for in-gel trypsin digestion followed by analysis of the peptides by liquid chromatography coupled to mass spectrometry (Materials and Methods). Table 1 lists the identity of the proteins, their molecular weight, their annotated function, whether they are predicted to bind pyridine nucleotides, and whether they are essential for mycobacterial growth in liquid culture. Table 1 of the Supporting Information gives additional information, including the accession numbers, the overall protein score, the number of unique peptides detected for each protein, the sequence and score for each unique peptide, and the sequence coverage for each protein in Table 1. We note that bands 1, 3, 5, 8, and 10 contain more than one protein species with similar molecular masses that were not resolved by SDS−PAGE (see Table 1).

DISCUSSION

Power of INH−NAD(P) Affinity Chromatography. Large amounts of *M. tuberculosis* cell extract are difficult to obtain because of the organism's highly infective nature, requiring high-level safety containment, and its unusually slow doubling time of 18−24 h. These realities present significant challenges to the performance of biochemical characterizations in this organism, and in this study, we were restricted to a total of approximately 400 mg of *M. tuberculosis* crude soluble protein cell extract for performing all the experiments presented in this paper. We developed a one-step INH−NAD(P) affinity chromatography purification method (see Materials and Methods) that permitted the highly selective purification and identification of proteins that bind INH−NAD(P) with high affinity (see below), which is similar to a general procedure that has recently been introduced (*29*). The known three-dimensional structures of the 4*S*-isonicotinoyl−NAD adduct bound to InhA and the 4*R*-isonicotinoyl−NADP adduct bound to DHFR revealed that in these two known targets, there are essentially no interactions between the exocyclic adenine amine of the adducts and the enzyme (*8*, *13*). We thus elected to covalently couple the

Table 1: High-Affinity INH−NAD(P)-Binding Proteins from *M. tuberculosis* H37Rv

band	Rv	gene	MW	annotated function[a]	pyridine nucleotide binding?	essential?[b]
1	Rv3248c	SahH	54 324	*S*-adenosylhomocysteine hydrolase	yes	yes
	Rv0753c	MmsA	54 454	methylmalonic acid semialdehyde dehydrogenase	yes	no
	Rv1187	RocA	58 841	pyrroline-5-carboxylate dehydrogenase	yes	yes
2	Rv0155	PntAA	37 694	proton-translocating transhydrogenase α-subunit	yes	unknown
3	Rv2623		31 652	universal stress protein (similar to Rv1996)	unknown	yes
	Rv1996		33 880	universal stress protein (similar to Rv2623)	unknown	no
	Rv0468	FadB2	30 728	3-hydroxybutyryl-CoA dehydrogenase	yes	no
4	Rv1484	InhA	28 528	enoyl-ACP reductase	yes	yes[c]/no[b]
5	Rv2691	CeoB/TrkA	24 240	NAD^+-binding subunit of the potassium uptake protein complex	yes	no
	Rv0091	Mtn/Sah	27 340	bifunctional 5′-methylthioadenosine/*S*-adenosylhomocysteine nucleosidase	no	no
6	Rv2858c	AldC	48 259	aldehyde dehydrogenase	yes	unknown
7	Rv1059		36 910	unknown (similar to Rv0926c)	unknown	unknown
8	Rv0926c		37 751	unknown (similar to Rv1059)	unknown	no
	Rv3777		33 963	probable oxidoreductase	yes	no
9	Rv2971		30 364	probable oxidoreductase	yes	yes
10	Rv2766c	FabG5	27 140	3-oxoacyl-ACP reductase	yes	no
	Rv2671	RibD	27 694	bifunctional deaminase/reductase involved in riboflavin biosynthesis	yes	no
11	Rv2763c	DfrA	17 640	dihydrofolate reductase	yes	yes[d]/unknown[b]

[a] Tuberculist (http://genolist.pasteur.fr/TubercuList/). [b] From ref *49*. [c] From ref *10*. [d] From ref *55*.

adducts via this position using *N*-hydroxysuccinamide-activated Sepharose (Materials and Methods). From 100 mg of *M. tuberculosis* crude soluble protein cell extract, approximately 50 μg of total protein was recovered from solid supports containing the covalently coupled INH−NAD(P) adducts. This amount of protein, specifically eluted by the identical adduct pool that was covalently bound to the columns, was sufficient to obtain the identity of all the protein bands in the two silver-stained gels shown in Figure 2. We note that because of the stereochemically uncontrolled nature of the nonenzymatic reaction between activated isoniazid and pyridine nucleotides, as well as the subsequent spontaneous, but reversible, cyclization of the acyclic forms [compounds **1** and **4** (Figure 1)] to generate the corresponding cyclic forms [compounds **2**, **3**, **5**, and **6** (Figure 1)], the proteins we isolated could, in principle, bind any of the six isomers of INH−NAD(P) shown in Figure 1.

INH−NAD(P) Affinity Chromatography Is Highly Selective. To determine the selectivity of our approach, we analyzed the final INH−NAD(P) protein eluates from the INH−NAD(P)−Sepharose and $NAD(P)^+$−Sepharose columns by SDS−PAGE followed by silver staining (Figure 2). Most of the proteins that bind to the INH−NAD(P) columns are unique when compared to the corresponding proteins that bind to the $NAD(P)^+$−Sepharose control columns [lane 2 vs lane 1 and lane 4 vs lane 3 (Figure 2)], demonstrating the high selectivity of this method for the proteins of interest. In addition, the profile of proteins bound to the columns containing covalently bound INH−NAD is completely different from that of the INH−NADP column [lane 2 vs lane 4 (Figure 2)] as expected, since most dehydrogenases are specific for either the nonphosphorylated (NADH) or phosphorylated (NADPH) forms of the pyridine nucleotides. Finally, band 4, which is the most intense band in lane 2, was unambiguously identified as InhA, a known and validated target of INH. Moreover, even though no silver-stained band is observed within the box marked 11 in lane 4, probably reflecting its low cellular abundance, we excised this gel slice because it corresponds to the position in the gel where DHFR was expected to migrate, and we detected a single DHFR tryptic peptide with a high score from this region after in-gel digestion. The isolation of InhA and DHFR, the only two *M. tuberculosis* proteins known to bind INH−NAD(P) adducts with subnanomolar to low nanomolar affinity (*7*, *13*), demonstrates that the method is successful at isolating the known high-affinity INH−NAD(P)-binding proteins. We note that identification of the proteins in the final INH−NAD(P) eluates from the $NAD(P)^+$−Sepharose control columns was not attempted as these proteins appear to have a high affinity for $NAD(P)^+$ since the prior 1 mM $NAD(P)^+$ wash was not sufficient to remove them from the columns. Thus, endogenous $NAD(P)^+$ is expected to protect these proteins from INH−NAD(P) inhibition in vivo.

INH has also been proposed to target the *kasA*-encoded β-ketoacyl ACP synthase (*30*). This enzyme is also a component of the fatty acid synthase II complex, and it catalyzes the condensation of malonyl-ACP with acyl-ACP during each elongation cycle of fatty acid biosynthesis. The observation of a covalent complex of KasA, AcpM, and INH in isoniazid-treated *M. tuberculosis* led to the proposal that KasA was the primary target for INH (*30*). We note that since the KasA-catalyzed reaction is not pyridine nucleotide-dependent, it is not surprising that we did not isolate this protein using our method.

High-Affinity INH−NAD(P)-Binding Proteins. Of the 18 proteins listed in Table 1, only InhA and DHFR have previously been demonstrated to be inhibited by INH−NAD(P). Nine others are predicted to be pyridine nucleotide-dependent dehydrogenases/reductases. SahH (Rv3248c), which encodes *S*-adenosylhomocysteine hydrolase, is not a dehydrogenase/reductase but uses a tightly bound pyridine nucleotide coenzyme, which cycles between the NAD^+ and NADH oxidation states, to catalyze the cleavage of the homocysteine moiety of *S*-adenosylhomocysteine (*31*−*33*). The sequence of CeoB/TrkA (Rv2691) is 24% identical with

that of the *Escherichia coli* TrkA protein, which encodes the NAD^+-binding subunit of the potassium transport system. It is interesting to note that the *M. tuberculosis* CeoB/TrkA gene had previously been identified in a novel selection for INH resistance in an *E. coli* oxyR strain, which is more susceptible to INH and hydrogen peroxide than the parent strain (*34*). The open reading frames, Rv0926c and Rv1059, the sequences of which are 32% identical, have unknown function, but examination of the two aligned amino acid sequences shows that they have a GXGXXG amino acid motif (*35*) near their N-termini, an indicator that they could bind pyridine nucleotides.

As with any method, it is likely that there will be some false positives. Rv2623 and Rv1996, for example, the sequences of which are 40% identical, are predicted to be universal stress proteins, which bind and hydrolyze ATP (*36*). A large body of evidence suggests that Rv2623 is important for the nonreplicating persistence state of *M. tuberculosis*. Rv2623 has been shown to be induced under hypoxic conditions (*37*, *38*), in standing cultures (*39*), upon macrophage phagocytosis (*40*), and during lung infection (*41*). *M. tuberculosis* has been termed "the world's most successful pathogen" in part because of its ability to persist inside the human host for years or decades without causing fulminant disease, resulting in the infection of one-third of the human population (*42*). It is possible that Rv2623 and Rv1996 were identified using our method because they bind to the ADP portion of the INH−NAD inhibitor. However, their absence in lane 1 (Figure 2) and the probability that they would have been removed in the 1 mM NAD^+ wash suggest that this is unlikely. Expression and purification of these proteins are required to verify their annotated function as well as their ability to bind INH−NAD. Finally, Mtn/Sah (Rv0091), which encodes a bifunctional 5′-methylthioadenosine/*S*-adenosylhomocysteine nucleosidase, does not use pyridine nucleotides as substrates. It is possible that it has high affinity for a protein that binds to INH−NAD−Sepharose, for example, *S*-adenosylhomocysteine hydrolase (above), resulting in the copurification of these two proteins as a complex. Again, expression and purification of Mtn/Sah are required to determine if it has the ability to independently bind to, and be inhibited by, INH−NAD.

Pleiotropic Effects of INH. An important as yet unanswered question is which of the 12 INH−NAD(P) adducts are the active forms of the drug. Mutations in the promoter region and within the structural gene of *inhA* have been identified in INH-resistant *M. tuberculosis* clinical isolates that confer low-level resistance to isoniazid (*15*, *43*, *44*). Since InhA binds the acyclic 4*S* isomer of the INH−NAD adduct [compound **1** (Figure 1)], one might argue that this or one of its two equilibrating cyclic forms [compounds **2** and **3** (Figure 1)] is the bactericidal species and that the remaining nine adducts, although they do form in vivo, do not inhibit significantly any other essential enzyme in vivo. However, these mutations confer only low-level resistance to isoniazid (*15*, *43*, *44*). In addition, the purified recombinant InhA structural mutants still bind tightly and are inhibited potently by compound **1** ($K_i^* = 2.3-5.3$ nM) (*7*), suggesting that the mechanism of action of isoniazid is more complex than simply inhibiting a single enzyme target.

INH has previously been shown to inhibit mycolic acid (*45*−*47*) and nucleic acid biosynthesis in vitro (*48*). INH has also been proposed to affect NAD^+ and pyridoxal phosphate metabolism by acting as an antimetabolite of these coenzymes (*2*, *47*). In addition to InhA and DHFR, we have found 16 other enzymes that bind tightly to and could be inhibited by INH−NAD(P). These are involved in an extraordinary variety of cellular processes, including *S*-adenosylmethionine-dependent methyl transfer (SahH, see below), pyrimidine and valine catabolism (MmsA), the arginine degradative pathway (RocA), proton and potassium transport (PntAA and CeoB/TrkA, respectively), stress response (Rv2623 and Rv1996), lipid metabolism (FadB2 and FabG5), riboflavin biosynthesis (RibD), and various pyridine nucleotide-dependent redox reactions of unknown biochemical function (AldC, Rv3777, and Rv2971). The high-density mutagenesis study of Sasseti et al. (*49*), which identified candidate genes required for normal growth but which require individual confirmation, suggests that four of these new targets (SahH, Rv2623, Rv2971, and Rv1187) are essential for optimum growth of *M. tuberculosis* in vitro (*49*). We note that some genes which are not essential for mycobacterial growth in vitro may be essential for growth in vivo. Thus, INH has multiple targets, and it may be that the simultaneous inhibition of these multiple enzymatic targets results in the thoroughly documented bactericidal effects of INH treatment, resulting in cell lysis.

Inhibition of a specific cellular process by INH could also be the result of inhibition of multiple enzymes involved in the same biosynthetic process. Inhibition of mycolic acid biosynthesis, for example, has been credited to inhibition of InhA (*10*, *15*) or KasA (*30*), both of which are components of the type II fatty acid synthase complex (*9*). Mycolic acids are decorated with various functional groups, including cyclopropyl, keto, and methoxy groups, which are essential for *M. tuberculosis* survival within macrophages (*11*, *12*). The methoxy groups are introduced by *S*-adenosylmethionine-dependent methyltransferases (*12*). Since most methyltransferases are product-inhibited by *S*-adenosylhomocysteine, cells have evolved *S*-adenosylhomocysteine hydrolase (SahH and Rv3248c), to keep the cellular levels of *S*-adenosylhomocysteine low (*32*, *33*). We suggest that by inhibiting SahH, the INH−NAD adduct would indirectly interfere with these essential steps in mycolic acid maturation. We have recently proposed that inhibition of nucleic acid biosynthesis by INH results from inhibition of DHFR by INH−NADP (*48*). By inhibiting SahH, INH would additionally, though indirectly, inhibit the methyltransferases involved in the methylation of uracil and cytosine residues in tRNA by the accumulation of *S*-adenosylhomocysteine.

CONCLUSIONS

The single-drug/single-target paradigm of most antibiotics may not apply to INH. There are 12 INH−pyridine nucleotide metabolites (*6*), each one potentially targeting a different enzyme. We demonstrate here that there are at least 18 proteins that bind INH−NAD(P) adducts with high affinity. There may be even more proteins in the *M. tuberculosis* proteome that we failed to isolate and identify because they may not be sufficiently abundant, they may be expressed only in vivo, or they may be sterically prevented from binding because of the covalent attachment of INH−NAD(P) via the exocyclic adenine amine to the solid support. We believe that this study will encourage gene knockout

studies of the genes we have identified here to determine if they are essential for in vitro and in vivo growth of *M. tuberculosis*. We also believe that this study may assist in guiding the identification of mutations, within the genes we identified, in *M. tuberculosis* INH-resistant clinical isolates for which the genotypes are unknown (*15*).

The treatment of tuberculosis involves the co-administration of four drugs, most of which are synthetic compounds specific to the treatment of this human disease. Many of these, like isoniazid, are pro-drugs (*15*), including ethionamide (*50*, *51*), pyrazinamide (*52*), and the nitroimidazole, PA-824 (*53*), which is being tested for its activity against the persisting population of organisms (*54*). In many cases, scant evidence exists for the active form of the drug, or its intracellular mycobacterial target. The emergence of multidrug-resistant (isoniazid- and rifampicin-resistant) clinical isolates is threatening the effectiveness of these few compounds, forcing clinicians to resort to less effective, more toxic, and more expensive treatment options. The proteins and enzymes that we have identified in this study appear to provide promising new candidates for biochemical- and structure-based inhibitor design that could lead to new therapeutic approaches for the control and eradication of tuberculosis.

ACKNOWLEDGMENT

RawFileExtractor is an in-house script written by Dr. Christopher Paulse. *M. tuberculosis* H37Rv whole cell lysate was received as part of the National Institutes of Health and National Institute of Allergy and Infectious Disease Contract HHSN266200400091C, entitled Tuberculosis Vaccine Testing and Research Materials, which was awarded to the Colorado State University. Michael Yu provided guidance with in-gel trypsin digests.

SUPPORTING INFORMATION AVAILABLE

Proteomic analysis of INH−NAD(P)-binding proteins (Table 1). This material is available free of charge via the Internet at http://pubs.acs.org.

REFERENCES

1. Bernstein, J., Lott, W. A., Steinberg, B. A., and Yale, H. L. (1952) Chemotherapy of experimental tuberculosis. V. Isonicotinic acid hydrazide (nydrazid) and related compounds, *Am. Rev. Tuberc. 65*, 357−364.
2. Youatt, J. (1969) A review of the action of isoniazid, *Am. Rev. Respir. Dis. 99*, 729−749.
3. Bloom, B. R., and Murray, C. J. (1992) Tuberculosis: Commentary on a reemergent killer, *Science 257*, 1055−1064.
4. Zhang, Y., Heym, B., Allen, B., Young, D., and Cole, S. (1992) The catalase-peroxidase gene and isoniazid resistance of *Mycobacterium tuberculosis*, *Nature 358*, 591−593.
5. Banerjee, A., Dubnau, E., Quemard, A., Balasubramanian, V., Um, K. S., Wilson, T., Collins, D., de Lisle, G., and Jacobs, W. R., Jr. (1994) *InhA*, a gene encoding a target for isoniazid and ethionamide in *Mycobacterium tuberculosis*, *Science 263*, 227−230.
6. Nguyen, M., Claparols, C., Bernadou, J., and Meunier, B. (2001) A fast and efficient metal-mediated oxidation of isoniazid and identification of isoniazid-NAD(H) adducts, *ChemBioChem 2*, 877−883.
7. Rawat, R., Whitty, A., and Tonge, P. J. (2003) The isoniazid-NAD adduct is a slow, tight-binding inhibitor of InhA, the *Mycobacterium tuberculosis* enoyl reductase: Adduct affinity and drug resistance, *Proc. Natl. Acad. Sci. U.S.A. 100*, 13881−13886.
8. Rozwarski, D. A., Grant, G. A., Barton, D. H., Jacobs, W. R., Jr., and Sacchettini, J. C. (1998) Modification of the NADH of the isoniazid target (InhA) from *Mycobacterium tuberculosis*, *Science 279*, 98−102.
9. White, S. W., Zheng, J., Zhang, Y. M., and Rock, C. O. (2004) The structural biology of type II fatty acid biosynthesis, *Annu. Rev. Biochem.* 791−831.
10. Vilcheze, C., Morbidoni, H. R., Weisbrod, T. R., Iwamoto, H., Kuo, M., Sacchettini, J. C., and Jacobs, W. R., Jr. (2000) Inactivation of the InhA-encoded fatty acid synthase II (FAS II) enoyl-acyl carrier protein reductase induces accumulation of the FAS I end products and cell lysis of *Mycobacterium smegmatis*, *J. Bacteriol. 182*, 4059−4067.
11. Barry, C. E., III, Lee, R. E., Mdluli, K., Sampson, A. E., Schroeder, B. G., Slayden, R. A., and Yuan, Y. (1998) Mycolic acids: Structure, biosynthesis and physiological functions, *Prog. Lipid Res. 37*, 143−179.
12. Takayama, K., Wang, C., and Besra, G. S. (2005) Pathway to synthesis and processing of mycolic acids in *Mycobacterium tuberculosis*, *Clin. Microbiol. Rev. 18*, 81−101.
13. Argyrou, A., Vetting, M. W., Aladegbami, B., and Blanchard, J. S. (2006) *Mycobacterium tuberculosis* dihydrofolate reductase is a target for isoniazid, *Nat. Struct. Mol. Biol. 13*, 408−413.
14. Miller, G. P., and Benkovic, S. J. (1998) Stretching exercises: Flexibility in dihydrofolate reductase catalysis, *Chem. Biol. 5*, R105−R113.
15. Zhang, Y., Vilcheze, C., and Jacobs, W. R., Jr. (2005) in *Tuberculosis and the Tubercle Bacillus* (Cole, S. T., Eisenach, K. D., McMurray, D. N., and Jacobs, W. R., Jr., Eds.) pp 115−140, ASM Press, Washington, DC.
16. Cole, S. T., Brosch, R., Parkhill, J., Garnier, T., Churcher, C., Harris, D., Gordon, S. V., Eiglmeier, K., Gas, S., Barry, C. E., III, Tekaia, F., Badcock, K., Basham, D., Brown, D., Chillingworth, T., Connor, R., Davies, R., Devlin, K., Feltwell, T., Gentles, S., Hamlin, N., Holroyd, S., Hornsby, T., Jagels, K., Krogh, A., McLean, J., Moule, S., Murphy, L., Oliver, K., Osborne, J., Quail, M. A., Rajandream, M. A., Rogers, J., Rutter, S., Seeger, K., Skelton, J., Squares, R., Squares, S., Sulston, J. E., Taylor, K., Whitehead, S., and Barrell, B. G. (1998) Deciphering the biology of *Mycobacterium tuberculosis* from the complete genome sequence, *Nature 393*, 537−544.
17. Miesel, L., Weisbrod, T. R., Marcinkeviciene, J. A., Bittman, R., and Jacobs, W. R., Jr. (1998) NADH dehydrogenase defects confer isoniazid resistance and conditional lethality in *Mycobacterium smegmatis*, *J. Bacteriol. 180*, 2459−2467.
18. Vilcheze, C., Weisbrod, T. R., Chen, B., Kremer, L., Hazbon, M. H., Wang, F., Alland, D., Sacchettini, J. C., and Jacobs, W. R., Jr. (2005) Altered NADH/NAD^+ ratio mediates coresistance to isoniazid and ethionamide in mycobacteria, *Antimicrob. Agents Chemother. 49*, 708−720.
19. Pasca, M. R., Guglierame, P., De Rossi, E., Zara, F., and Riccardi, G. (2005) *mmpL7* gene of *Mycobacterium tuberculosis* is responsible for isoniazid efflux in *Mycobacterium smegmatis*, *Antimicrob. Agents Chemother. 49*, 4775−4777.
20. Alland, D., Kramnik, I., Weisbrod, T. R., Otsubo, L., Cerny, R., Miller, L. P., Jacobs, W. R., Jr., and Bloom, B. R. (1998) Identification of differentially expressed mRNA in prokaryotic organisms by customized amplification libraries (DECAL): The effect of isoniazid on gene expression in *Mycobacterium tuberculosis*, *Proc. Natl. Acad. Sci. U.S.A. 95*, 13227−13232.
21. Wilson, M., DeRisi, J., Kristensen, H. H., Imboden, P., Rane, S., Brown, P. O., and Schoolnik, G. K. (1999) Exploring drug-induced alterations in gene expression in *Mycobacterium tuberculosis* by microarray hybridization, *Proc. Natl. Acad. Sci. U.S.A. 96*, 12833−12838.
22. Betts, J. C., McLaren, A., Lennon, M. G., Kelly, F. M., Lukey, P. T., Blakemore, S. J., and Duncan, K. (2003) Signature gene expression profiles discriminate between isoniazid-, thiolactomycin-, and triclosan-treated *Mycobacterium tuberculosis*, *Antimicrob. Agents Chemother. 47*, 2903−2913.
23. Boshoff, H. I., Myers, T. G., Copp, B. R., McNeil, M. R., Wilson, M. A., and Barry, C. E., III (2004) The transcriptional responses of *Mycobacterium tuberculosis* to inhibitors of metabolism: Novel insights into drug mechanisms of action, *J. Biol. Chem. 279*, 40174−40184.
24. Waddell, S. J., Stabler, R. A., Laing, K., Kremer, L., Reynolds, R. C., and Besra, G. S. (2004) The use of microarray analysis to determine the gene expression profiles of *Mycobacterium tuberculosis* in response to anti-bacterial compounds, *Tuberculosis 84*, 263−274.

25. Hughes, M. A., Silva, J. C., Geromanos, S. J., and Townsend, C. A. (2006) Quantitative proteomic analysis of drug-induced changes in mycobacteria, *J. Proteome Res. 5*, 54−63.
26. Smith, P. K., Krohn, R. I., Hermanson, G. T., Mallia, A. K., Gartner, F. H., Provenzano, M. D., Fujimoto, E. K., Goeke, N. M., Olson, B. J., and Klenk, D. C. (1985) Measurement of protein using bicinchoninic acid, *Anal. Biochem. 150*, 76−85.
27. Ducasse-Cabanot, S., Cohen-Gonsaud, M., Marrakchi, H., Nguyen, M., Zerbib, D., Bernadou, J., Daffe, M., Labesse, G., and Quemard, A. (2004) In vitro inhibition of the *Mycobacterium tuberculosis* β-ketoacyl-acyl carrier protein reductase MabA by isoniazid, *Antimicrob. Agents Chemother. 48*, 242−249.
28. Lei, B., Wei, C. J., and Tu, S. C. (2000) Action mechanism of antitubercular isoniazid. Activation by *Mycobacterium tuberculosis* KatG, isolation, and characterization of InhA inhibitor, *J. Biol. Chem. 275*, 2520−2526.
29. Oda, Y., Owa, T., Sato, T., Boucher, B., Daniels, S., Yamanaka, H., Shinohara, Y., Yokoi, A., Kuromitsu, J., and Nagasu, T. (2003) Quantitative chemical proteomics for identifying candidate drug targets, *Anal. Chem. 75*, 2159−2165.
30. Mdluli, K., Slayden, R. A., Zhu, Y., Ramaswamy, S., Pan, X., Mead, D., Crane, D. D., Musser, J. M., and Barry, C. E., III (1998) Inhibition of a *Mycobacterium tuberculosis* β-ketoacyl ACP synthase by isoniazid, *Science 280*, 1607−1610.
31. Palmer, J. L., and Abeles, R. H. (1979) The mechanism of action of *S*-adenosylhomocysteinase, *J. Biol. Chem. 254*, 1217−1226.
32. Kloor, D., and Osswald, H. (2004) *S*-Adenosylhomocysteine hydrolase as a target for intracellular adenosine action, *Trends Pharmacol. Sci. 25*, 294−297.
33. Stepkowski, T., Brzezinski, K., Legocki, A. B., Jaskolski, M., and Bena, G. (2005) Bayesian phylogenetic analysis reveals two-domain topology of *S*-adenosylhomocysteine hydrolase protein sequences, *Mol. Phylogenet. Evol. 34*, 15−28.
34. Chen, P., and Bishai, W. R. (1998) Novel selection for isoniazid (INH) resistance genes supports a role for NAD^+-binding proteins in mycobacterial INH resistance, *Infect. Immun. 66*, 5099−5106.
35. Wierenga, R. K., Terpstra, P., and Hol, W. G. (1986) Prediction of the occurrence of the ADP-binding $\beta\alpha\beta$-fold in proteins, using an amino acid sequence fingerprint, *J. Mol. Biol. 187*, 101−107.
36. Kvint, K., Nachin, L., Diez, A., and Nystrom, T. (2003) The bacterial universal stress protein: Function and regulation, *Curr. Opin. Microbiol. 6*, 140−145.
37. Boon, C., Li, R., Qi, R., and Dick, T. (2001) Proteins of *Mycobacterium bovis* BCG induced in the Wayne dormancy model, *J. Bacteriol. 183*, 2672−2676.
38. Rosenkrands, I., Slayden, R. A., Crawford, J., Aagaard, C., Barry, C. E., III, and Andersen, P. (2002) Hypoxic response of *Mycobacterium tuberculosis* studied by metabolic labeling and proteome analysis of cellular and extracellular proteins, *J. Bacteriol. 184*, 3485−3491.
39. Florczyk, M. A., McCue, L. A., Stack, R. F., Hauer, C. R., and McDonough, K. A. (2001) Identification and characterization of mycobacterial proteins differentially expressed under standing and shaking culture conditions, including Rv2623 from a novel class of putative ATP-binding proteins, *Infect. Immun. 69*, 5777−5785.
40. Monahan, I. M., Betts, J., Banerjee, D. K., and Butcher, P. D. (2001) Differential expression of mycobacterial proteins following phagocytosis by macrophages, *Microbiology 147*, 459−471.
41. Shi, L., Jung, Y. J., Tyagi, S., Gennaro, M. L., and North, R. J. (2003) Expression of Th1-mediated immunity in mouse lungs induces a *Mycobacterium tuberculosis* transcription pattern characteristic of nonreplicating persistence, *Proc. Natl. Acad. Sci. U.S.A. 100*, 241−246.
42. Hingley-Wilson, S. M., Sambandamurthy, V. K., and Jacobs, W. R., Jr. (2003) Survival perspectives from the world's most successful pathogen, *Mycobacterium tuberculosis*, *Nat. Immunol. 4*, 949−955.
43. Basso, L. A., Zheng, R., Musser, J. M., Jacobs, W. R., Jr., and Blanchard, J. S. (1998) Mechanisms of isoniazid resistance in *Mycobacterium tuberculosis*: Enzymatic characterization of enoyl reductase mutants identified in isoniazid-resistant clinical isolates, *J. Infect. Dis. 178*, 769−775.
44. Musser, J. M. (1995) Antimicrobial agent resistance in mycobacteria: Molecular genetic insights, *Clin. Microbiol. Rev. 8*, 496−514.
45. Winder, F. G., and Collins, P. B. (1970) Inhibition by isoniazid of synthesis of mycolic acids in *Mycobacterium tuberculosis*, *J. Gen. Microbiol. 63*, 41−48.
46. Takayama, K., Wang, L., and David, H. L. (1972) Effect of isoniazid on the *in vivo* mycolic acid synthesis, cell growth, and viability of *Mycobacterium tuberculosis*, *Antimicrob. Agents Chemother. 2*, 29−35.
47. Quemard, A., Lacave, C., and Laneelle, G. (1991) Isoniazid inhibition of mycolic acid synthesis by cell extracts of sensitive and resistant strains of *Mycobacterium aurum*, *Antimicrob. Agents Chemother. 35*, 1035−1039.
48. Gangadharam, P. R., Harold, F. M., and Schaefer, W. B. (1963) Selective inhibition of nucleic acid synthesis in *Mycobacterium tuberculosis* by isoniazid, *Nature 198*, 712−714.
49. Sassetti, C. M., Boyd, D. H., and Rubin, E. J. (2003) Genes required for mycobacterial growth defined by high density mutagenesis, *Mol. Microbiol. 48*, 77−84.
50. DeBarber, A. E., Mdluli, K., Bosman, M., Bekker, L. G., and Barry, C. E., III (2000) Ethionamide activation and sensitivity in multidrug-resistant *Mycobacterium tuberculosis*, *Proc. Natl. Acad. Sci. U.S.A. 97*, 9677−9682.
51. Baulard, A. R., Betts, J. C., Engohang-Ndong, J., Quan, S., McAdam, R. A., Brennan, P. J., Locht, C., and Besra, G. S. (2000) Activation of the pro-drug ethionamide is regulated in mycobacteria, *J. Biol. Chem. 275*, 28326−28331.
52. Scorpio, A., and Zhang, Y. (1996) Mutations in *pncA*, a gene encoding pyrazinamidase/nicotinamidase, cause resistance to the antituberculous drug pyrazinamide in tubercle bacillus, *Nat. Med. 2*, 662−667.
53. Stover, C. K., Warrener, P., VanDevanter, D. R., Sherman, D. R., Arain, T. M., Langhorne, M. H., Anderson, S. W., Towell, J. A., Yuan, Y., McMurray, D. N., Kreiswirth, B. N., Barry, C. E., and Baker, W. R. (2000) A small-molecule nitroimidazopyran drug candidate for the treatment of tuberculosis, *Nature 405*, 962−966.
54. Barry, C. E., III, Boshoff, H. I., and Dowd, C. S. (2004) Prospects for clinical introduction of nitroimidazole antibiotics for the treatment of tuberculosis, *Curr. Pharm. Des. 10*, 3239−3262.
55. Suling, W. J., Reynolds, R. C., Barrow, E. W., Wilson, L. N., Piper, J. R., and Barrow, W. W. (1998) Susceptibilities of *Mycobacterium tuberculosis* and *Mycobacterium avium* complex to lipophilic deazapteridine derivatives, inhibitors of dihydrofolate reductase, *J. Antimicrob. Chemother. 42*, 811−815.

BI061874M